

Modern Sands Derived from the Vertiskos Unit of the Serbomacedonian Massif (N. Greece): a Preliminary Study on the Weathering of the Unit

Research Article

Ioannis K. Georgiadis^{1*}, Antonios Koroneos^{1†}, Ananias Tsirambides^{1‡}, Michael Stamatakis^{2§}

¹ Aristotle University of Thessaloniki, School of Geology,
Department of Mineralogy-Petrology-Economic Geology,
541 24 Thessaloniki, Greece

² National and Kapodistrian University of Athens, School of Geology and Geoenvironment,
Department of Economic Geology and Geochemistry,
157 84 Athens, Greece

Received 10 April 2012; accepted 6 July 2012

Abstract: Modern sand samples were collected from the Vertiskos Unit of the Serbomacedonian Massif, northern Greece, and were examined for their texture and mineralogical composition. They were collected from active channels and torrents. The textural study demonstrated that these modern sands are moderately to very-poorly sorted, often polymodal in grain size distribution, texturally and mineralogically immature to submature, and consist of coarse-grained gravelly sands to slightly-gravelly muddy sands. The dominant composition is quartzofeldspathic. All samples contain detrital minerals of metamorphic origin, mainly amphibole and garnet, in addition to minor amounts of pyroxene and detrital calcite. These sediments were deposited rapidly and close to their source, the metamorphic basement of the Vertiskos Unit. The mineral constituents of the samples indicate that the Vertiskos Unit is undergoing rapid physical weathering due to the temperate and seasonal climate. The results of this study suggest that these modern sands constitute one sedimentary petrologic province comprised of primarily of amphibole-garnet.

Keywords: Detrital • fluvial • immature • heavy minerals • PXRD

© Versita sp. z o.o.

1. Introduction

*E-mail: i.georgia@chem.auth.gr

†E-mail: koroneos@geo.auth.gr

‡E-mail: ananias@geo.auth.gr

§E-mail: stamatakis@geol.uoa.gr

The main processes leading to the formation and transport of sand-sized grains are [1]: weathering (including both disintegration and decomposition), explosive volcanism, crushing (not including ordinary abrasion), pelletization and precipitation from solution. In general, sands accumulate in high kinetic energy environments, such as stream channels, alluvial fans, and marine environments [2]. The

most important factors influencing the accumulation of sediment are the medium of transport and deposition, in addition to climate and source area. [3].

Studies on modern sands enhance the current understanding of the impact of processes responsible for the creation of sand-size sediment. This information can be used to interpret the paleogeography of the ancient source area and basin systems [4]. The factors that affect the texture and composition of detrital assemblages found in modern and ancient sediments include source-rock composition, tectonics, climate, and relief [5]. These factors, grouped together, are referred to as provenance [6]. In a more descriptive way, the provenance includes descriptions of the paleogeography of a region, the identification of possible source areas for the clastic material, and information about the paleocurrents and paleoslope [1]. Quaternary sediments are particularly useful in provenance studies, because the effects of diagenetic dissolution in these sediments are minor compared to ancient sandstones [7]. Analyses of the mineralogy of modern sands may elucidate valuable minerals that, if the provenance is better characterized, can be more accurately uncovered. [1]. Furthermore, petrographic studies of sand provide opportunities to develop better sampling procedures using a systematic quantitative approach [8].

Quaternary sediments from Doirani Lake (NW margin of Vertiskos Unit) are coarse- to medium-grained, poorly-sorted, feldspathic wackes and arkoses that were deposited in a lacustrine environment with little transportation as indicated by the presence of ferromagnesian minerals [9]. Drilling cuttings (fluvial sand gravels to gravel sands) from Hervo, Kilkis (West margin of Vertiskos Unit), are also mineralogically immature litharenites to feldspathic litharenites or orthoquartzites, formed by intense physical weathering with rapid transport and deposition in either a semi-arid climate or under the influence of a high relief [10]. The aforementioned detrital sediments are exclusively sourced from the metamorphic basement of the Vertiskos Unit. To the east of the Unit, the alluvial fans formed near Lake Kerkini are composed of clastic material derived from gneisses, amphibolites, and quartzites [11]. The following minerals are found in the sand fraction of clastic material accumulated to the east of the Unit: quartz, feldspars, micas, calcite, amphiboles, epidote, garnet, apatite, clinopyroxene and opaque minerals [12].

The detrital sediments studied are deposited on and around the basement and consist of soil profiles as well as generally loose fluvial formations. This preliminary study focuses on the textural, petrological and mineralogical study of modern sands from the Vertiskos Unit to determine the processes responsible for the formation of

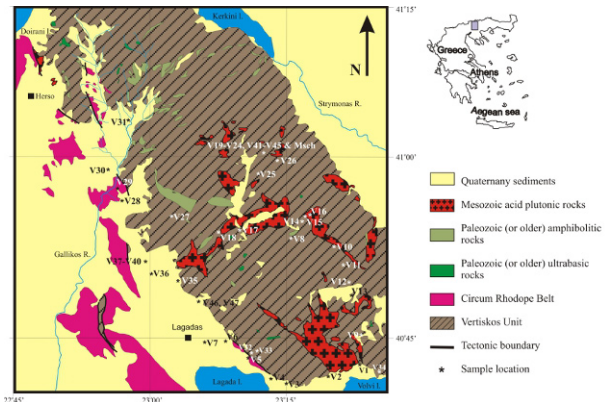


Figure 1. Petrographic sketch map of the study area (Vertiskos Unit), demonstrating the distribution of the samples.

these sediments, the potential source rocks, and current rate of weathering affecting the Unit using mechanical, petrographic and mineralogical techniques.

2. Geological setting

The study area is located in the Serbomacedonian Massif (SMM), northern Greece [13] and, more specifically, comprises the northern and largest part of the Vertiskos Unit [14, 15]. The SMM forms a zone of rocks approximately 600 km long and 60-100 km wide, trending to the N/NW (344°)-S/SE (132°), in the central part of The Balkan Peninsula. It is divided into three geomorphologic units, namely the Northern, the Central, and the Southern [16]. The Vertiskos (geotectonic) Unit studied here coincides with the northern part of the Southern (geomorphologic) Unit of the SMM. This area is characterized by intense relief created by mountain-horst and basin-graben structures [16].

The maximum altitude of the Vertiskos Unit is approximately 1,179 m and it is drained by several rivers and torrents. This complex drainage system is generally dendritic in nature, discharging its detrital load to Gallikos and Strymon Rivers (west and east ends of the Massif, respectively), to Doirani and Kerkini Lakes to the north and to Lagada and Volvi Lakes to the south (north and south ends of the Unit, respectively) (Fig. 1). The Unit generally demonstrates low relief creating gently sloping mountains and two mesas at 400-600 m and 600-800 m [16].

The Greek part of the SMM is divided into the upper Vertiskos Unit and the lower Kerdillia Unit [14, 15]. More recently, on the basis of lithological characteristics of the basement rocks, the SMM was further divided into several main Units, including Pirgadikia, Vertiskos, Arnea, and

Kerdillia [17]. The older definition [15] is used throughout this study.

The metamorphic basement of the Vertiskos Unit is mainly comprised of Palaeozoic metasediments and metabasic rocks, along with Eocene to Miocene granites. The Unit was metamorphosed during the Paleozoic to an amphibolite facies, and then underwent Cretaceous retrograde metamorphosis to a greenschist facies [18].

A more detailed analysis revealed the Unit is composed of the following lithologies [19–21]:

1. Meta-sediments (mica schists, meta-sandstones, meta-arkoses and marbles). These lithologies occupy the bulk of the study area. The marbles rarely occur as beds or lenses in the schists and demonstrate distinct stratigraphic contacts. Where a gradual transition exists between the mica schists and marbles, the transition zone between the two units consists of a rock with a unique composition. The meta-sediments are Palaeozoic and demonstrate a poly-metamorphic character [21, 22], rather than just the two metamorphic events described above [18]. This poly-phase metamorphism occurred during the Mesozoic [23].
2. Migmatites (Palaeozoic or older). They are found in thick intercalations within the mica schists. Usually the schists demonstrate a gradual transition to migmatites. Their protoliths must have been the aforementioned meta-sediments [19].
3. Amphibolites (Palaeozoic or older). They are thick and found interbedded between migmatites and mica schists, transitioning gradually between lithologies. These rocks are igneous in origin, probably from tholeiitic magma [24, 25].
4. Ultrabasic rocks (serpentinites and talc-chlorite schists). These outcrop throughout the Unit as lenses tectonically emplaced in mica schists. Their age is Palaeozoic or older.
5. Eclogites and amphibolitized eclogites (Paleozoic or older). They are found as lenses in mica schists with indistinct contacts due to the effects of deformation and erosion. Eclogites studied from the southern part of the Unit bear evidence of high pressure metamorphism and suggest a transitional basalt type protolith [26].
6. Acid plutonic rocks. These rocks are generally known as the Arnea Granite Suite [22] and their age is Jurassic to Tertiary [27].

7. Pegmatites. They are found as veins in mica schists and amphibolites. Their age is Jurassic to Tertiary [28, 29].

8. Small occurrences of Tertiary acid volcanic rocks.

9. Poorly sorted Tertiary massive graywackes along with poorly sorted and massive arkoses [30].

The principal rock types of the Vertiskos Unit are deformed orthogneisses that likely metamorphosed from medium-grained porphyritic biotite-granite preserved in strain-free pockets in the orthogneisses [23]. The orthogneisses are associated with amphibolites and low-grade metasediments, the latter present only to the west of the SMM and to in the central interior [17]. To the West the meta-sediments are in tectonic contact with the Circum Rhodope Belt, a low-grade metamorphic volcano-sedimentary succession [31]. The meta-sediments of the western border of the SMM likely metamorphosed from potassic arkoses and graywackes of mixed provenance, including igneous and sedimentary [32].

Five metamorphic episodes affected the Vertiskos Unit. They are illustrated in the P-T diagram of Fig. 2 [19, 20]: M₁ episode. Hercynian age (Devonian or prior), P>9kb, 400°C<T<550°C. It is represented by the eclogites.

M₂ episode. Hercynian age (Devonian), 3.5kb<P<8.5kb, 650°C<T<750°C. It is represented by the meta-sediments, migmatites, and amphibolites. Amphibolitization of the eclogites begins.

M₃ episode. Permo-Triassic age, 5kb<P<8kb and 500°C<T<690°C. Amphibolitization of the eclogites continues.

M₄ episode. Late Jurassic age, 6kb<P<9kb, 400°C<T<520°C. Extensive serpentinization of the ultrabasic rocks takes place.

M₅ episode. Post Jurassic age, low metamorphic grade. Based on the ultrabasic rocks of the Unit it is deduced that the pressure and temperature conditions were P≤5kb and 300°C<T<500°C, respectively, whereas the amphibolitized eclogites demonstrated T≤440°C.

For a more detailed overview of the metamorphic evolution of the SMM, the reader is referred to more recent studies [23, 33, 34].

Strong evidences of neotectonic activity are recorded on the Vertiskos Unit [16]. The basin-grabens of the Unit were developed in two stages [35]: the first occurred during Lower-Middle Miocene and the second during Upper Pliocene-Lower Pleistocene; both due to the active extension in the central Aegean area. Neotectonic activity continues today as high seismicity and earthquakes with shallow focal depth (<17 km) [16]. The SMM as a whole is characterised by an active tectonic lineament of NNW-SSE direction with a N-S extensional trend [36–38].

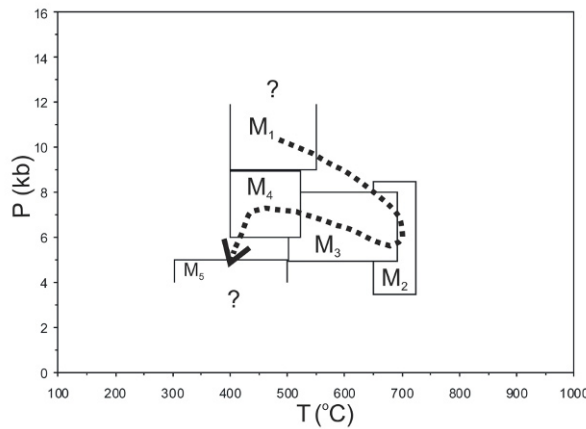


Figure 2. P-T path of the rocks comprising the Vertiskos Unit.

The total thickness of the Neogene and Quaternary deposits in the smaller grabens and the larger basins ranges from 500–1500 m and 1500–3500 m, respectively. This feature indicates very active exogenic processes, producing almost planar surfaces onto the Vertiskos Unit [16]. Palynological study of drill cores from Lake Doirani, NW border of the Vertiskos Unit, revealed that after ca 830 BC the area was affected by intense human activity and that erosion of the surrounding rocks increased, producing more sand and gravel [39]. Based on this data, it is estimated that in this region, Vertiskos Unit is yielding sediments of approximate thickness 0.11 cm/yr.

3. Materials and Methods

Forty seven spot samples [40] of modern sands and soils were collected at different location within and around the Vertiskos Unit, labelled V1 to V47. Moist samples were left to dry at room temperature and then separated into consecutive size fractions by sieving in order to examine their textural properties using graphical parameters. Powder X-ray diffraction (PXRD) was used to determine the mineralogical composition of the samples.

Powder X-ray diffraction was performed on a Philips diffractometer with Ni-filtered $\text{CuK}\alpha$ radiation. Randomly oriented mounts of the chemically untreated samples were scanned over the interval $3\text{--}63^\circ 2\theta$ at a scanning speed of 1.2° per minute. The gravel fraction was removed prior to the grinding. Semi-quantitative estimates of the minerals present are based on the use of zinc oxide (zincite, PDF card 79-0207) as an internal standard [41]. The sample was prepared by grinding 3 g of dried sand in an agate mortar with 0.333 g ZnO and 4 ml CH_3OH . The mixture is then dried at 85°C for one hour and scanned.

In addition, the petrography of thins sections of 0 Φ , 1 Φ , and 2 Φ size fractions was completed as the majority of particles this size consist of preserved rock fragments [42]. Below approximately 3 Φ there are virtually no rock fragments. Thin sections were created by agglomerating loose grains in a compact block using a polyester resin; this process allowed for the shape of the grains along with the distribution of minerals in each fraction to be examined.

4. Results

4.1. Texture and Lithology

At the macroscopic level all modern sand samples are typically brown and reddish-grey-coloured coarse-grained loose sands consisting of sandy gravel to gravelly sand with little to no mud. However, Samples V19 to V24 and V41 to V45, which are soils immediately overlying the mica schist basement, contain a higher percentage of mud. In addition, macroscopic grains are typically angular to subangular with a low sphericity; the more rounded lithic fragments in this size population are of metamorphic origin, usually schist. Some rounded granite pebbles are also found in the samples collected from the center of the Unit, generally not exceeding approximately 10 cm in size. The statistical graphical parameters relative to the grain size populations of the sand samples analysed are presented in Table 1. The statistical equations utilized and their associated interpretations are according to [43]. Figure 3 shows some representative grain-size distributions, illustrating the polymodal nature of the grain size populations. Figure 4 shows the textural classification of the samples studied [43]. Figures 5 and 6 provide an image of the two sampling locations; whereas, Figure 7 segregates the environment of deposition [44].

According to the variation in amplitude of the inclusive graphic standard deviation, σ_i ; samples V15, V16, V18 and V33 appear to be moderately sorted while samples V19, V21, V22, V24, V25, V30, V31 and V39 are very poorly sorted. The remaining samples are poorly sorted [43].

The degree of sorting along and mud content in the samples suggest that the sands are texturally immature to submature [43, 45]. The textural immaturity of the samples was expected from their grain distribution. The inclusive graphic skewness, S_{ki} , shows that grain-size curves range from extremely coarse skewed to extremely fine skewed, with the majority of the samples yielding a symmetrical grain size distribution.

The samples demonstrate graphic kurtosis ranging from 0.65 to 1.54, very platykurtic to very leptokurtic, respectively, with the majority of them mesokurtic.

Table 1. Statistical parameters of grain size populations of the modern sands analyzed.

Sample	G	M	S	M_o	M_d	M_Z	QD_ϕ	σ_l	Sk_l	K_G	C
V1	44.8	0.8	54.4	-1.06, 1.80, 4.05	-0.74	-0.49	1.41	1.82	1.17	0.83	-3.60
V2	48.6	0.7	50.7	-1.33, 1.29	-0.75	-0.41	1.29	1.82	0.21	0.92	-3.80
V3	34.1	0.1	65.8	-0.54	-0.59	-0.59	0.87	1.33	-0.07	1.06	-3.90
V4	43.2	0.6	56.1	-0.90	-0.76	-0.62	1.23	1.69	0.08	0.88	-3.90
V5	48.0	0.4	51.5	-2.42, -0.58	-0.97	-0.92	1.27	1.68	0.02	0.86	-3.95
V6	57.4	0.5	42.1	-3.44, -1.29	-1.36	-1.35	0.99	1.52	-0.02	1.04	-3.95
V7	30.8	0.4	68.8	-0.08	-0.25	-0.21	1.09	1.59	-0.003	0.97	-3.50
V8	27.7	0.2	72.1	-3.54, 0.29	-0.14	-0.41	1.01	1.68	-0.29	1.11	-3.95
V9	37.2	0.3	62.4	-0.76	-0.68	-0.55	0.85	1.31	0.10	1.08	-3.00
V10	28.8	0.5	70.7	-2.40, 0.40	0.03	-0.19	1.14	1.64	-0.18	0.91	-3.60
V11	38.9	0.2	60.9	-1.22, 1.15	-0.57	-0.34	1.24	1.68	0.13	0.88	-3.50
V12	50.2	0.6	49.0	-1.63, 0.90	-1.08	-0.75	1.29	1.84	0.22	0.93	-3.80
V13	14.8	2.3	83.0	1.87	1.00	0.94	1.21	1.79	-0.10	0.99	-3.40
V14	17.0	0.3	82.7	-1.45	-1.28	-1.12	0.70	1.11	0.16	1.18	-2.30
V15	33.6	0.1	66.2	-1.65	-1.70	-1.64	0.62	0.97	-0.02	1.04	-2.60
V16	27.3	0.1	72.6	-0.60	-0.55	-0.48	0.65	0.97	0.04	1.01	-2.40
V17	22.3	0.2	77.6	-0.18	-0.29	-0.26	0.71	1.04	0.00	0.98	-2.10
V18	28.3	0.4	71.3	-0.62	-0.58	-0.50	0.63	0.99	0.05	1.05	-2.50
V19	8.1	32.6	59.3	1.94, 4.44	2.18	2.19	1.85	2.17	-0.11	0.74	-3.50
V20	3.9	37.0	59.1	0.75, 4.45	2.03	2.30	1.81	1.94	0.07	0.65	-3.00
V21	13.8	29.1	57.3	0.97, 2.85, 5.06	2.04	1.93	1.98	2.45	-0.18	0.79	-3.70
V22	6.8	55.0	38.2	0.50, 2.43, 4.45	4.07	3.02	1.79	2.10	-0.74	0.75	-3.50
V23	22.2	4.6	73.3	0.38	0.55	0.13	1.26	1.83	-0.01	0.95	-3.40
V24	21.0	3.7	75.3	-2.24, 0.54	0.77	0.78	1.35	2.06	-0.03	1.03	-3.80
V25	41.8	11.7	46.4	-2.24, 0.91, 3.03, 5.03	-0.45	-0.13	1.60	2.64	0.16	1.05	-3.90
V26	9.9	0.7	89.3	-3.49, 1.31	1.04	0.94	0.72	1.35	-0.30	1.54	-3.80
V27	37.3	0.8	61.9	-3.24, -0.03	-0.48	-0.58	1.22	1.77	-0.11	0.94	-3.90
V28	17.2	1.6	81.1	0.84	0.39	0.36	1.01	1.53	-0.10	1.08	-3.50
V29	27.2	0.9	71.9	0.33	0.00	-0.15	1.02	1.56	-0.13	1.02	-3.50
V30	27.4	4.0	68.6	-3.40, 0.53, 3.60	0.37	0.27	1.57	2.37	-0.08	0.97	-3.90
V31	40.0	13.2	46.7	-2.13, 2.36, 4.45	-0.45	-0.01	1.69	2.50	0.26	0.95	-3.80
V32	4.6	2.8	92.6	-3.42, 1.16	1.17	1.25	0.77	1.28	0.06	1.20	-3.30
V33	7.9	0.2	91.9	0.23	0.14	0.16	0.65	0.95	-0.02	1.03	-2.00
V34	29.4	0.3	70.2	-0.45	-0.41	-0.37	0.92	1.39	-0.01	1.05	-3.50
V35	42.9	1.2	55.8	-1.14	-0.74	-0.73	1.13	1.78	0.02	1.11	-3.90
V36	49.9	1.4	48.7	-1.48, 0.16	-1.00	-0.97	1.36	1.85	0.07	0.91	-3.90
V37	27.7	1.2	71.1	-3.33, 0.45	0.08	-0.07	1.05	1.68	-0.17	1.13	-3.80
V38	42.3	0.8	56.9	-1.36	-0.73	-0.54	1.03	1.51	0.15	1.05	-3.90
V39	28.4	5.5	66.0	-3.54, -1.23, 0.33	0.14	0.45	1.57	2.26	0.11	0.99	-3.90
V40	63.8	0.0	36.2	-1.76	-1.58	-1.40	1.08	1.54	0.14	0.95	-3.80
V41	30.5	68.6	0.9	0.33, 2.34	-0.18	-0.24	1.02	1.60	-0.03	1.12	-3.50
V42	17.0	81.1	1.9	0.36	0.19	0.25	0.87	1.34	0.07	1.05	-2.00
V43	28.7	0.8	70.5	-3.30, 0.44	0.07	0.03	1.25	1.81	-0.07	0.97	-3.80
V44	27.1	72.4	0.5	-0.01	-0.24	-0.19	0.91	1.35	0.05	1.01	-2.70
V45	24.0	1.7	74.3	0.25	0.00	0.08	0.96	1.53	0.09	1.08	-2.70
V46	65.2	0.8	34.0	-2.46	-1.92	-1.34	1.11	1.55	0.52	0.90	-3.10
V47	34.1	0.2	65.7	0.27	-0.30	-0.34	1.19	1.61	-0.10	0.88	-3.90

G=gravel (wt. %), M=mud (silt+clay) (wt. %), S=sand (wt. %), M_o =mode (ϕ), M_d =median (ϕ), M_Z =graphic mean (ϕ), QD_ϕ =quartile deviation at ϕ (ϕ), σ_l =inclusive graphic standard deviation (ϕ), Sk_l =inclusive graphic skewness, K_G =graphic kurtosis and C=one percentile (equals to ϕ_1).

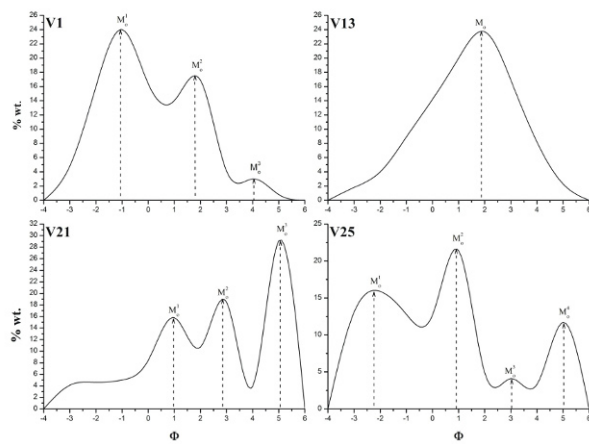


Figure 3. Representative grain size distributions of some samples studied. M_0 =mode of the grain population occurrence (Φ).



Figure 5. Sampling location of V6.

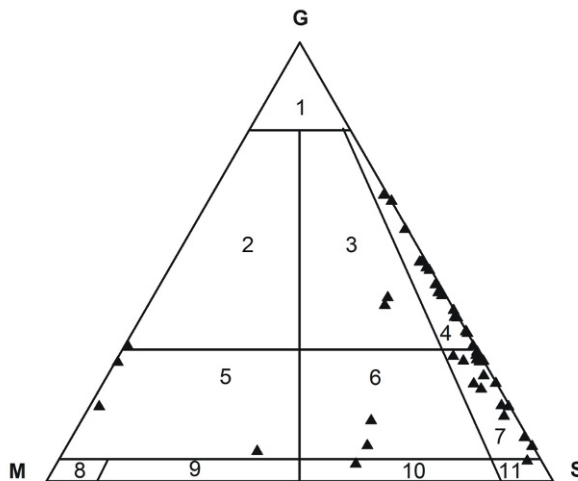


Figure 4. Textural classification of modern sand samples [43]. Apex symbols as in Table 1. Fields: 1=gravel, 2=muddy gravel, 3=muddy sandy gravel, 4=sandy gravel, 5=gravelly mud, 6=gravelly muddy sand, 7=gravelly sand, 8=slightly gravelly mud, 9=slightly gravelly sandy mud, 10=slightly gravelly sandy mud and 11=slightly gravelly sand.

However, caution should be exercised when making interpretations based on these results as the samples demonstrate a polymodal grain-size distribution. [43].

The samples shown in Figure 4 are classified as follows: V41 is muddy gravel; V25 and V31 are muddy sandy gravels; V1 -V7, V9, V11, V12, V15, V27, V35, V36, V38, V40, V46 and V47 are sandy gravels; V22, V42, and V44 are gravelly muds; V19 and V21 are gravelly muddy sands; V8, V10, V13, V14, V16, V17, V18, V23, V24, V26, V28-V30, V33, V34, V37, V39, V43 and V45 are gravelly sands; V20



Figure 6. Sampling location of V33.

is a slightly gravelly muddy sand; and V32 is a slightly gravelly sand [43].

The fluvial character of the majority of the samples is confirmed by the discrimination diagram illustrated in Figure 7.

4.2. Mineralogy and Petrology

The powder X-ray diffraction semi-quantitative mineralogical composition of the sand samples is shown in Table 2. The petrographic classification adopted is shown in Figure 8 [42]. In order to make the classification scheme applicable to bulk X-ray analyses, the percentages of quartz, total feldspars, and clay matrix were used rather than rock fragments. In this study, the total phyllosilicate content (micas+chlorite) of the samples was used as the clay matrix, since these are modern and loose sediments that were not affected by diagenesis and consolidation. In the pet-

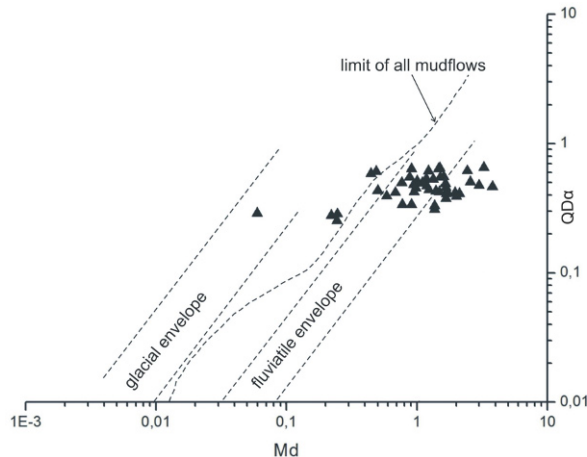


Figure 7. Discrimination diagram of the depositional environments of the samples studied.

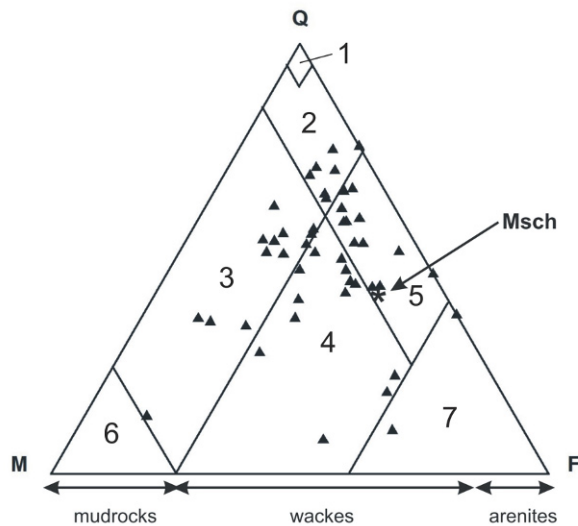


Figure 8. Ternary diagram for the classification of detrital sediments [42]. 1=orthogranite, 2=protoquartzite (quartzarenites), 3=quartz-wacke, 4=greywacke (phyllarenite), 5=arkose, 6=mudrock, 7=field beyond the maximum feldspar content observed, Msch=mica schist of the basement, Q=quartz, F=feldspars and M=micas+chlorite.

rographic classification scheme adopted in this study, the term greywacke is used for sandstones rich in micaceous (matrix) material. The term phyllarenites was used to indicate samples with a lower mud content [43]. Accessory minerals, those comprising greater than 3% of the mineral content of the sample, are included as prefixes to the rock naming.

The classification scheme used in this study is also useful as an indirect method for the designation of chemical and textural maturity of sand: chemical maturity increases

with increasing percentages of micas (or clay) and physical maturity increasing with increasing percentages of quartz. In this way, the fields of protoquartzite and arkose represent texturally mature (i.e. sands that contain less than 15% matrix) arenitic sands. Using this association, the fields of protoquartzite and quartz-wackes represent chemically mature sands, whereas the fields of arkoses and greywackes represent chemically immature sands [42].

In the ternary diagram shown in Figure 8, an estimated composition of the mica schist (average of three samples) of the basement is also plotted for comparison. In the same figure, samples V1 and V24 plot outside the limit of 60% total feldspar; however, with their close proximity to this limit and the semi-quantitative nature of this estimate they closely approach, they were incorporated to the arkoses and phyllarenites (greywackes) groups, respectively.

The powder X-ray diffraction examination reveals that the samples have a diverse composition with the quartz content ranging from 7% to 70%. Other compositional variations were observed in the plagioclase content (8-54%), alkali feldspar content (0-42%), and mica content (0-73%). In addition, accessory ferromagnesian minerals (i.e. amphiboles and pyroxenes) and detrital garnet and calcite are almost always present in the composition of the samples. On occasion, amphibole occurs in great amounts (e.g. samples V12 and V22, Table 2).

All of samples presented in this study are mineralogically immature, as they contain feldspars, ferromagnesian minerals, and heavy minerals (i.e. micas, amphibole, pyroxene and garnet) [45]. This can be attributed to rapid erosion and mixing of sand populations from different, but adjacent, sources.

According to the petrographic classification scheme adopted in this study (Fig. 8), the samples may be classified into four groups, including A) Quartz-arenites: samples V3, V7, V9, V10, V26, V29 and V30; B) Quartz-wackes: samples V2, V6, V8, V25, V28, V31, V35, V38, V39, V40, V41, V42 and V45; C) Phyllarenites: samples V4, V5, V12, V14, V20, V23, V24, V27, V32, V33, V36, V37, V43 and V44; and D) Arkoses: samples V1, V11, V13, V15, V16, V17, V18, V19, V21, V22, V34, V46 and V47.

Figure 9 shows representative photomicrographs of some samples are presented. The 1 Φ fraction assemblage consists mainly of monocrystalline and polycrystalline quartz, plagioclase always altered to sericite, few alkali feldspar usually found as orthoclase, and individual euhedral crystals of muscovite, biotite, or along quartz. The Quartz present exhibits undulatory extinction and, when present in fine quartzose aggregates, shows characteristic lobe sutures. Individual quartz and feldspar crystals

Table 2. Mineralogical composition (wt. %) and classification of the modern sands analyzed.

Sample	Q	Pl	Kf	M	Am	Px	G	Cc	Classification
V1	35	20	42		4				Am-arkosic sandy gravel
V2	13	13		73			1		quartz-wacky sandy gravel
V3	70	16	8		5		1		Am-quartz-arenitic sandy gravel
V4	40	24	13	19		2		1	phyllarenitic sandy gravel
V5	45	33	3	16	1		2		phyllarenitic sandy gravel
V6	48	15	3	22	3	2		7	quartz-wacky sandy gravel
V7	70	19	2	8					quartz-arenitic sandy gravel
V8	39	13	4	20	18	2	4		G-Am-quartz-wacky gravelly sand
V9	55	17	6	11	6	1	1	3	Am-quartz-arenitic sandy gravel
V10	65	8	15	12					quartz-arenitic gravelly sand
V11	35	37	12		17				Am-arkosic sandy gravel
V12	27	23	3	20	27				Am-phyllarenitic sandy gravel
V13	41	34	7	3	12	3			Am-arkosic gravelly sand
V14	20	51	3	17	9				Am-phyllarenitic gravelly sand
V15	49	27	6	11	2	3	2		arkosic sandy gravel
V16	43	29	15	12	2				arkosic gravelly sand
V17	60	22	5	10		2			arkosic gravelly sand
V18	63	13	13	8	1	1		1	arkosic gravelly sand
V19	31	27	12	10	13	1	6		G-Am-arkosic gravelly muddy sand
V20	16	54		19	2		6	3	G-phyllarenitic slightly gravelly muddy sand
V21	46	24	10	9	7	1	2		Am-arkosic gravelly muddy sand
V22	37	21	5	7	28	1	1		Am-arkosic gravelly mud
V23	7	44	5	38	2	1	2		phyllarenitic gravelly sand
V24	9	48	12	22		2	8		G-phyllarenitic gravelly sand
V25	50	12	3	28	5	2			Am-quartz-wacky muddy sandy gravel
V26	66	12	6	10	4	2			Am-quartz-arenitic gravelly sand
V27	49	27		20	1	2	1		phyllarenitic sandy gravel
V28	49	22	2	20	4	2			Am-quartz-wacky gravelly sand
V29	70	17	1	5	4	1			Am-quartz-arenitic gravelly sand
V30	66	15	2	13	4				Am-quartz-arenitic gravelly sand
V31	55	21	3	20		1			quartz-wacky muddy sandy gravel
V32	48	29	5	16		2	1		phyllarenitic slightly gravelly sand
V33	43	26	12	17	2	1	1		phyllarenitic gravelly sand
V34	60	18	9	6	5	1	2		Am-arkosic gravelly sand
V35	25	10	2	10		3	50		Cc-quartz-wacky sandy gravel
V36	43	34	5	17			1		phyllarenitic sandy gravel
V37	47	24	2	26					phyllarenitic gravelly sand
V38	48	21		26	3		1		quartz-wacky sandy gravel
V39	33	11	3	46	3		4		G-quartz-wacky gravelly sand
V40	53	22	2	18	2	2	1		quartz-wacky sandy gravel
V41	29	18	3	37	4	2	7		Am-G-quartz-wacky muddy gravel
V42	43	12	5	26	12		2		Am-quartz-wacky gravelly mud
V43	23	24	3	37	10		3		Am-phyllarenitic gravelly sand
V44	32	11	18	29	5	3	1		Am-phyllarenitic gravelly mud
V45	34	9	3	49	2		4		G-quartz-wacky gravelly sand
V46	54	24	5	11	3	2	1		arkosic sandy gravel
V47	57	24	8	8	2		1		arkosic sandy gravel
MSch	43	27	10	14			6		Mica schist (Palaeozoic basement)

Q=quartz, Pl=plagioclase, Kf=alkali feldspars, M=micas including chlorite, Am=amphibole, Px=pyroxene, G=garnet, Cc=calcite and MSch=mean composition of the mica schist of the basement.

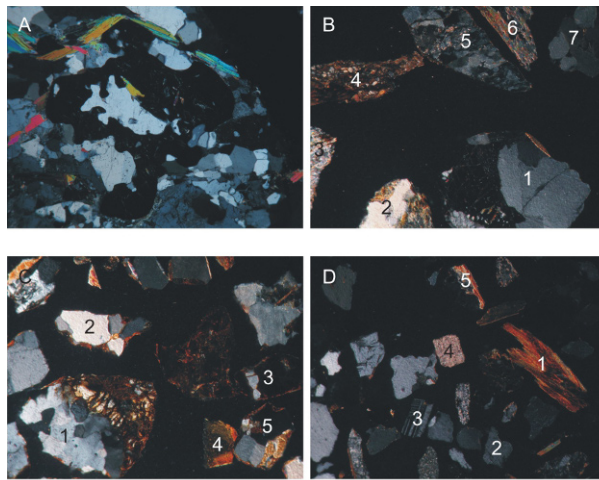


Figure 9. A) Photomicrograph of the mica schist of the basement. Allotropic garnet crystal with quartz and white mica crystals. Porphyroblastic texture. The horizontal dimension of the picture equals to about 2 mm. Nicol+. B) Photomicrograph of fraction 0 ϕ from sample V26. 1=rock fragment with undulatory quartz and garnet, 2=rock fragment with undulatory quartz, fine biotite and fine white mica, 3=fragment with fine white mica, 4=rock fragment with biotite and quartz, 5=polycrystalline fine quartz with minor white mica, 6=muscovite fragment and 7=polycrystalline quartz. Nicol+. C) Photomicrograph of fraction 1 ϕ from sample V19. 1=rock fragment with undulatory quartz, biotite and garnet, 2=rock fragment with undulatory quartz and biotite, 3=rock fragment with quartz and biotite crystal showing extinction, 4=monocrystalline biotite and 5=rock fragment with quartz and amphibole. Nicol+. D) Photomicrograph of fraction 1 ϕ from sample V25, 1=biotite crystals, 2=alkali feldspar single crystal, 3=plagioclase single crystal showing twinning, 4=rock fragment with fine white mica and 5=rock fragment containing amphibole crystal. Nicol+.

are generally angular to subangular. Opaque minerals are always present in small amounts. Other accessory minerals found are individual euhedral garnet and kyanite crystals and single orthopyroxene and rutile crystals. Rock fragments are generally subangular to subrounded, and composed of quartz, biotite, muscovite, amphibole, plagioclase, epidote, kyanite, sillimanite, and zoisite. In these fragments, quartz demonstrates characteristic lobe sutures. The texture and composition of the rock fragments indicates that the mica schist basement is the likely source. The Michel-Levy method was applied to three plagioclase crystals demonstrating albite twinning along the (010) plane perpendicular to the thin section in the 1 ϕ fraction of sample V19. The results of this analysis suggest that these plagioclase have an acid composition (albite). This type of composition is found in plagioclase from low grade metamorphic rocks and pegmatites [46]. In the 2 ϕ fraction, the amount of rock fragments decreases and becomes more angular, however, the mineralogical composition remains the same. This fraction is rich in sin-

gle angular to subangular crystals of muscovite, orthopyroxene, epidote, biotite, kyanite, plagioclase (altered in sericite), quartz, orthoclase, clinopyroxene, garnet, rutile, and some amphibole. The 3 ϕ fraction consists primarily of single angular crystals of the aforementioned minerals, plus minor amounts of zoisite.

In general, their high content in lithic fragments and feldspars implies an adjacent source for the clastic load [47].

5. Discussion

In general, the samples analyzed demonstrate unimodal to polymodal grain-size distribution patterns and are moderately sorted to very poorly sorted. The former indicating that they are immature to submature [43]. This feature is indicative of sediments accumulated through rapid deposition close to their source or of weak current action (i.e. detrital material deposited from a viscous flow, such as a mud flow) [43, 47]. The first conclusion point also implies that these sediments were deposited under intense to mild tectonic activity [43].

Fluvial sediments demonstrate $\sigma_1 > 1.2\phi$ (or sometimes $> 1.3\phi$) and $Sk_1 < 1$ (rarely > 1), whereas flood plain sediments demonstrate mostly $\sigma_1 > 2\phi$ and always $Sk_1 < 1$ [48]. This rule is not always followed by the samples studied. In general, the samples studied are arenitic and wacky in texture.

In Figure 7, samples V19, V20, V21, V26 and V32 plot as mud flows. For the first three this would be expected, since they are soil samples rich in fine-grained material. The latter two, being gravelly sands, only marginally plot outside the field of fluvial deposits.

The petrographic analysis of the samples shows that quartz is present in all samples, but its content varies greatly. Its presence is due to its abundance in the surrounding metamorphosed rocks and granites and to its mechanical resistance [49]. The texture of the quartzose rock fragments, as revealed from the polarized microscopy, is indicative of a metamorphic gneissic source: quartz crystals show undulatory extinction and intercrystalline suturing in polycrystalline grains. Also, assuming a first-cycle origin of the modern sands, the fine monocrystalline quartz grains must have originated from foliated metamorphic rocks [50].

The most altered feldspars in feldspathic sediments are the calcic ones and the least altered are the potassic [50], a general rule that seems to apply to all the samples studied. It is believed that feldspar grains breakdown by fracturing along twin crystal planes as they are transported in streams of high gradient [51]. In the samples

studied, feldspars do accumulate in the finer sand fractions but they also contribute to the coarser size fractions; this observation also supports the assumption that these sediments rapidly accumulated near their source.

Micas almost always comprise some percentage of the composition of the samples. Their abundance is due to the presence of mica in the metamorphic parent rocks. Chlorite was also detected in trace amounts in some of the samples along with some kaolinite. Their presence is associated with the alteration of micas and feldspars, respectively.

Varying amounts of detrital calcite was detected in some samples. This can be attributed to the minor amounts of carbonate rocks that outcrop in the Vertiskos Unit. Pyroxene, when detected, always comprises a minor amount of the samples analyzed. Garnet is a more common accessory mineral in the examined sands. The same is also true for amphiboles. All the three previous mentioned minerals are indicative of a metamorphic source and belong to the metastable group of heavy minerals [43]. In general, the abundances of garnet and pyroxene tend to decline with increased alluvial storage [52]. The heavy mineral assemblages in sandstones are affected by physical sorting, mechanical abrasion, and dissolution. Moreover, the source-area weathering does not significantly affect the diversity of heavy mineral suites that will be incorporated into the transport system, the degree of enrichment of stable heavy minerals being greatest in transport-limited erosional regimes [53]. The latter also favours the hypothesis that these sediments accumulated near their source.

The majority of the soil mass of the samples V19 to V24 and V41 to V45 (soils immediately overlying the mica schist basement), is residual. However, it is evident that the adjacent amphibolites contributed clastic material (significant presence of amphibole).

Because the samples studied are loose, sand-sized sediments and because they are rich in quartz feldspar, and occasionally heavy minerals, the question of whether or not these sediments have economic potential is raised. Further study is necessary in order to answer this question.

The framework composition and compositional maturity of fluvial sandstones, in addition to the climate setting, can be correlated [54, 55]; the more feldspathic (immature) were deposited near the source under a warm and dry climate and the more quartzose and mature were deposited under a wet climate. Under a semi-arid to Mediterranean (hot summer) climate plutoniclastic sands produced are less altered than under temperate and humid [56] conditions. This could indicate that the samples studied, due to their quartz content, may have been deposited under a wet climate where chemical weathering pervasive. The

samples studied were deposited in a semi-arid climate and were coupled by the effects of strong topographic relief [57]. The presence of feldspar and heavy minerals in the samples supports the latter hypothesis (temperate and seasonable climate where erosion is primarily due to physical weathering). Previous studies have also shown that the presence of amphibole and pyroxene in modern sediments is correlated with mild climatic conditions [58]. The presence of unstable minerals (i.e. pyroxene, plagioclase) along with semi-stable ones (i.e. amphibole, orthoclase) also suggests that chemical weathering did not play a role in sediment production [59].

All the sand samples studied comprise a distinct petrologic province correlated by age (modern), origin (metamorphic basement), and distribution. This province could be further characterized by an amphibole association including all the modern sand samples of the Vertiskos Unit [50].

6. Conclusions

The samples analyzed are generally brown and reddish-grey coloured, loose, fluvial sands, that demonstrate, at the macroscopic level, low sphericity, are angular to sub-angular. More rounded lithic fragments found in the samples are metamorphic in origin. Most of the samples yield a polymodal grain-size distribution. Texturally, they are moderately sorted to very poorly sorted and immature to submature. They are mainly sandy gravels and gravelly sands.

They are sediments that accumulated close to their source under intense to mild tectonic activity, under rapid weathering, and comprise a diverse mixture of detrital populations.

Their assemblage is composed mainly of quartz, feldspars, micas, and accessory minerals, mainly of metamorphic origin. The studied sands are feldspathic and rich in heavy minerals, namely amphibole and garnet. The latter feature supports the assertion that these sands are deposited close to their source. The composition of all samples indicates that their source was the Vertiskos Unit, mainly the mica schist and amphibolite layers.

The mineral abundances indicate that the Vertiskos Unit was rapidly weathered in a temperate and seasonable climate primarily through the action of physical weathering. In general, samples become more quartzose and depleted in accessory minerals further from their source.

All the samples constitute a distinct sedimentary petrologic province on the Unit comprised of an amphibole-garnet association.

Acknowledgements

The first author would like to thank Professor A. Filippidis and Lecturer N. Kantiranis for their help on powder X-ray diffraction analysis and the technicians G. Michailidis and D. Katsikas for the preparation of the thin sections. The first author is also grateful to Efxinos Leschi of Thessaloniki for the financial aid. The critical remarks of the anonymous reviewers are thankfully acknowledged.

References

- [1] Pettijohn F.J., Potter P.E., Siever R., *Sand and sandstone*. Springer-Verlag, New York, 1987
- [2] Ehlers E.G., Blatt H., *Petrology: Igneous, sedimentary and metamorphic*. W.H. Freeman and Co, San Francisco, 1982
- [3] Reineck H.-E., Singh I.B., *Depositional sedimentary environments*, 2nd ed. Springer-Verlag, New York, 1986
- [4] Dickinson W.R., Interpreting provenance relations from detrital modes of sandstones. In: Zuffa G.G. (Ed.), *Provenance of Arenites*. Reidel Publ, Dordrecht, 1985, 333–361
- [5] Suttner L.J., Sedimentary petrographic provinces: an evaluation. In: Ross C.A. (Ed.), *Paleogeographic provinces and provinciality*. SEPM Society for Sedimentary Geology, Tulsa, 1974, 75–84
- [6] Dickinson W.R., Interpreting detrital modes of greywacke and arkose. *J. Sediment. Petrol.*, 1970, 40, 695–707
- [7] Garzanti E., Ando S. Heavy mineral concentration in modern sands: implications for provenance interpretation. In: Mange M.A., Wright D.T. (Eds), *Heavy minerals in use*. Elsevier BV, 2007, 517–545
- [8] Weltje G.J., A quantitative approach to capturing the compositional variability of modern sands. *Sediment. Geol.*, 2004, 171, 59–77
- [9] Tsirambides A.E., Study of the Quaternary sediments of Doirani basin. *Ann. Geol. Pays Hell.* 1997, 37, 907–919 (in Greek with English abstract)
- [10] Georgiadis I.K., Tsirambides A., Kassoli-Fournarakis A., Trontsios G., Petrology and provenance study of the Quaternary clastic sediments from Hervo Kilkis (Macedonia, Greece). *Bull. Geol. Soc. Greece*, 2007, 40(2), 747–758
- [11] Papaflippou-Pennou E., Dynamic evolution and recent exogenic processes of Strymon network in Serres graben (North Greece). PhD Thesis, Aristotle University of Thessaloniki, Greece, 2004 (in Greek with English summary)
- [12] Vouvalidis K., Morphological, sedimentological, oceanographic processes and anthropogenic interventions that contribute to the evolution of the mouth system of Strymonas River. PhD Thesis, Aristotle University of Thessaloniki, Greece, 1998 (in Greek with English summary)
- [13] Kockel F., Walther H., Strimonline als Grenze zwischen Serbo-Mazedonischen und Rila-Rhodope Massiv in Ost-Mazedonien. *Geol. Jahrb.*, 1965, 83, 575–602
- [14] Kockel F., Mollat H., Walther H.W., Geologie des Serbo-Mazedonischen Massivs und seines mesozoischen Rahmens (Nordgriechenland). *Geol. Jahrb.*, 1971, 89, 529–551
- [15] Kockel F., Mollat H., Walther H.W., Erläuterungen zur geologischen Karte der Chalkidiki und angrenzender Gebiete 1:100000 (Nord-Griechenland). Bundesanstalt für Geowissenschaften und Rohstoffe, Hannover, 1977
- [16] Psilovikos A., Geomorphological and structural modification of the Serbomacedonian Massif during the neotectonic stage. *Tectonophysics*, 1984, 110, 27–45
- [17] Himmerkus F., Anders B., Reischmann T., Kostopoulos D.K., Gondwana-derived terranes in the northern Hellenides. In: Hatcher Jr. R.D., Carlson M.P., McBride J.H., Martínez-Catalán J.R. (Eds.), 4-D Framework of Continental Crust. Geological Society of America, Boulder, 2007, 379–390
- [18] Mountrakis D., Tectonic evolution of the Hellenic orogen: Geometry and kinematics of deformation. *Bull. Geol. Soc. Greece*, 2002, 34(6), 2113–2126
- [19] Kourou A.N., Lithology, geochemistry, tectonics and metamorphosis of a part of the Western part of Vertiskos group. The area NE of the Lake of Agios Vasilios (Koronia). PhD Thesis, Aristotle University of Thessaloniki, Greece, 1991 (in Greek with English summary)
- [20] Sidiropoulos N., Lithology, geochemistry, tectonics and metamorphosis of the Northwestern part of Vertiskos group. The area of Mountain Disoro (Kroussia), North of Kilkis. PhD Thesis, Aristotle University of Thessaloniki, Greece, 1991 (in Greek with English summary)
- [21] I.G.M.E., Sheet Lachanas. Geological map of Greece (1:50,000). Athens, Greece, 1979
- [22] Dixon J.E., Dimitriadis S., The metamorphic evolution of the Serbomacedonian Massif in Greece. *Terra Cognita*, 1987, 7, 106
- [23] Himmerkus F., Reischmann T., Kostopoulos D., Serbo-Macedonian revisited: A Silurian basement terrane from northern Gondwana in the Internal Hellenides, Greece. *Tectonophysics*, 2009, 471, 20–35

[24] Kassoli-Fournaraki A., The origin of the Kerdyllia series amphibolites (eastern Serbomacedonian mass), Greece. *N. Jb. Miner. Mh.*, 1982, 6, 272-278

[25] Papadopoulos C., Geologie des Serbomacedonischen Massivs nordlich des Volvi Sees (Nord Griecheland). Dissertation, University of Wien, Austria, 1982

[26] Dimitriadis S., Godelitsas A., Evidence for high pressure metamorphism in the Vertiskos Group of the Serbomacedonian Massif: The eclogite of Nea Roda, Chalkidiki. *Bull. Geol. Soc. Greece*, 1991, 25(2), 67-80

[27] Christofides G., Koroneos A. Pe-Piper G., Katirtzoglou K., Chatzikirkou A., Pre-Tertiary magmatism in the Serbomacedonian Massif (N. Greece): Kerkini granitic complex. *Bull. Geol. Soc. Greece*, 1999, 33, 131-148

[28] Marakis G. Geochronology on granites of Macedonia. *Ann. Geol. Pays Hellen.*, 1969, 21, 121-152 (in Greek with English abstract)

[29] Zervas S.A., Geochronology with the ^{87}Rb - ^{87}Sr method of some pegmatite samples from the area of Lagada. *Ann. Geol. Pays Hellen.*, 1980, 30, 143-153 (in Greek with English abstract)

[30] Chatzidimitriadis E., Tsirambides A., Theodorikas S., Clay mineral abundance of shales and slates from some Greek regions through geologic time. *Proc. Academy Athens*, 1993, 68, 144-161

[31] Kauffmann G., Kockel F., Mollat H., Notes on the stratigraphic and palaeogeographic position of the Svuola Formation in the innermost zone of the Hellenides (Northern Greece). *B. Soc. Geol. Fr.*, 1976, 18, 225-230

[32] Veranis N., Kougoulis Ch., Kassoli-Fournaraki A., The Examili Formation and its relation to the Vertiskos Subzone of the Serbomacedonian Massif. *Bull. Geol. Soc. Greece*, 1990, 22, 71-86

[33] Kiliias A., Falalakis G., Mountrakis D., Cretaceous-Tertiary structures and kinematics of the Serbomacedonian metamorphic rocks and their relation to the exhumation of the Hellenic hinterland (Macedonia, Greece). *Int. J. Earth Sci.*, 1999, 88, 513-531

[34] Meinhold G., Kostopoulos D., Frei D., Himmerkus F., Reischmann T., U-Pb LA-SF-ICP-MS zircon geochronology of the Serbo-Macedonian Massif, Greece: palaeotectonic constraints for Gondwanaderived terranes in the Eastern Mediterranean. *Int. J. Earth Sci. (Geol. Rundsch.)*, 2010, 99, 813-832

[35] Psilovikos A., Palaeogeographic evolution of the basin and the lake of Mygdonia (Lagada-Volvi). PhD Thesis, Aristotle University of Thessaloniki, Greece, 1977 (in Greek with English summary)

[36] Voidomatis Ph.S., Pavlides S.B., Papadopoulos G.A., Active deformation and seismic potential in the Serbomacedonian zone, northern Greece. *Tectonophysics*, 1990, 179, 1-9

[37] Pavlides S.B., Kondopoulou D.P., Kiliias A.A., Westphal M., Complex rotational deformations in the Serbo-Macedonian massif (north Greece): structural and paleomagnetic evidence. *Tectonophysics*, 1988, 145, 329-335

[38] Zagorchev I., Late Cenozoic development of the Strouma and Mesta fluviolacustrine systems, SW Bulgaria and Northern Greece. *Quaternary. Sci. Rev.*, 2007, 26, 2783-2800

[39] Athanasiadis N., Tonkov S., Atanassova J., Bozilova E., Palynological study of Holocene sediments from Lake Doirani in northern Greece. *J. Paleolimnol.*, 2000, 24, 331-342

[40] Krumbein W.C., Pettijohn F.J., Manual of sedimentary petrography. SEPM Reprint Series No 13, Tulsa, 1988

[41] Srodon J., Drits V.A., McCarty D.K., Hsieh J.C.C., Eberl D.D., Quantitative X-ray diffraction analysis of clay-bearing rocks from random preparations. *Clay Clay Miner.*, 2001, 49, 514-528

[42] Selley R.C., Applied sedimentology, 2nd ed. Academic Press, San Diego, 2000

[43] Folk R.L., Petrology of sedimentary rocks. Hemphill Publ. Co., Texas, 1974

[44] Buller A.T., McManus J., The application of quartile deviation-median diameter curves to the interpretation of sedimentary rocks. *J. Geol. Soc. London*, 1974, 130, 78-83

[45] Weller J.M., Stratigraphic principles and practises, Harper & Row, New York, 1960

[46] Deer W.A., Howie R.A., Zussman J., An introduction to the rock-forming minerals, 2nd ed. Longman, Essex, 1998

[47] Tucker M.E., Sedimentary petrology, 3rd ed. Blackwell, Oxford, 2001

[48] Fuchtbauer H., Muller G., Sediment – petrologie. Teil II Sedimente und sedimentgesteine. E. Schweizerbart'sche Verlagsbuchhandlung, Stuttgart, 1970

[49] Blatt H., Sedimentary petrology. Freeman & Co, New York, 1992

[50] Blatt H., Middleton G., Murray R., Origin of sedimentary rocks. Prentice-Hall Inc., New Jersey, 1972

[51] Pittman E.D., Destruction of plagioclase twins by stream transport. *J. Sediment. Petrol.*, 1969, 39, 1432-1437

[52] Morton A.C., Johnsson M.J., Factors influencing the composition of detrital heavy mineral suites in Holocene sands of the Apure River drainage basin, Venezuela. In: Johnsson M.J., Basu A. (Eds.), Pro-

cesses controlling the composition of clastic sediments. Geological Society of America, Boulder, 1993, 171–185

[53] Morton A.C., Hallsworth C.R., Processes controlling the composition of heavy mineral assemblages in sandstones. *Sediment. Geol.*, 1999, 124, 3–29

[54] Suttner L.J., Basu A., Mack G.H., Climate and the origin of quartz arenites. *J. Sediment. Petrol.*, 1981, 51, 1235–1246

[55] Suttner L.J., Dutta P.K., Alluvial sandstone composition and paleoclimate, I. Framework mineralogy. *J. Sediment. Petrol.*, 1986, 56(3), 329–345

[56] Girty G.H., A note on the composition of plutoniclastic sand produced in different climatic belts. *J. Sediment. Petrol.*, 1991, 61(3), 428–433

[57] von Eynatten H., Petrography and chemistry of sandstones from the Swiss Molasse Basin: An archive of the Oligocene to Miocene evolution of the Central Alps. *Sedimentology*, 2003, 50, 703–724

[58] Tsirambides A.E., Mineralogical composition of soils from Platamonas Pierias (Macedonia, Greece). *Bull. Geol. Soc. Greece*, 1999, 33, 99–104 (in Greek with English abstract)

[59] Garzanti E., Vezzoli G., Ando S., France-Lanord C., Singh S.K., Foster G., Sand petrology and focused erosion in collision orogens: The Brahmaputra case. *Earth Planet. Sc. Lett.*, 2004, 220, 157–174